Reorganization and in Vivo Dynamics of Microtubules during Arabidopsis Root Hair Development[w]

Nathalie Van Bruaene[1]*, Greg Joss, and Patrick Van Oostveldt

Laboratory for Biochemistry and Molecular Cytology, Ghent University, 9000 Gent, Belgium (N.V.B., P.V.O.); and Department of Biological Sciences, Macquarie University, Sydney, New South Wales 2109, Australia (G.J.)

Root hairs emerge from epidermal root cells (trichoblasts) and differentiate by highly localized tip growth. Microtubules (MTs) are essential for establishing and maintaining the growth polarity of root hairs. The current knowledge about the configuration of the MT cytoskeleton during root hair development is largely based on experiments on fixed material, and reorganization and in vivo dynamics of MTs during root hair development is at present unclear. This in vivo study provides new insights into the mechanisms of MT (re)organization during root hair development in Arabidopsis (*Arabidopsis thaliana*). Expression of a binding site of the MT-associated protein-4 tagged with green fluorescent protein enabled imaging of MT nucleation, growth, and shortening and revealed distinct MT configurations. Depending on the dynamics of the different MT populations during root hair development, either repeated two-dimensional (x, y, t) or repeated three-dimensional (x, y, z, t) scanning was performed. Furthermore, a new image evaluation tool was developed to reveal important data on MT instability. The data show how MTs reorient after apparent contact with other MTs and support a model for MT alignment based on repeated reorientation of dynamic MT growth.

A root hair is a long, lateral, tubular extension of an epidermal root cell formed by a process called tip growth. Diffuse longitudinal growth of the epidermal cell undergoes transition to highly localized and polarized growth at one specific site. After the formation of an initial bulge, the root hair grows by polarized exocytosis and deposition of cell wall material confined to the tip (Schnepf, 1986). In an early phase, 3-d-old Arabidopsis (*Arabidopsis thaliana*) root hairs grow out at a rate of 0.4 μm/min, followed by a late growth phase at 1 to 2.5 μm/min (Dolan et al., 1994). Tip growth is characterized by the presence of a vesicle-rich region, a reverse-fountain type of cytoplasmic streaming, and a gradient of cytoplasmic Ca^{2+} toward the hair tip (Pierson et al., 1996; Galway et al., 1997; Miller et al., 1997, 1999; Wymer et al., 1997; de Ruijter et al., 1998; Yang, 1998). During growth arrest cytoplasmic streaming switches from reverse-fountain streaming to circular streaming, and this reorganization is coupled to the disappearance of the vesicle-rich region (Miller et al., 1997).

It has been accepted that root hair outgrowth is associated with microtubule (MT) and actin filament reorientations (Emons and Derksen, 1986; Baluška et al., 2000). Bao et al. (2001) reported that reduced α-tubulin gene expression causes formation of multiple root hairs by single epidermal cells and ectopic root hair formation in tissues that are normally root hair free. This was the first evidence, to our knowledge, for a function of the MT cytoskeleton during root hair initiation, in particular suggesting a role for MT disassembly (caused by low α-tubulin expression) in the initiation of root hair formation. In maize (*Zea mays*) and lettuce (*Lactuca sativa*) the initiation of root hairs is associated with disorganization of the cortical-MT arrays in the trichoblast (Baluška et al., 2000; Takahashi et al., 2003a).

Filamentous actin plays a fundamental role in the tip growth process (for review, see Geitmann and Emons, 2000; Hepler et al., 2001). The function of MTs in tip growth is less clear and under debate. Both longitudinal and helical arrays of MTs have been described in root hairs (Lloyd, 1983; for review, see Geitmann and Emons, 2000) and do not seem to be part of the cellular machinery required for tip growth (Bibikova et al., 1999; Ketelaar et al., 2002). However, pharmacological studies showed that MTs are required to maintain growth directionality and unidirectional growth at the tip of root hairs (Bibikova et al., 1999; Ketelaar et al., 2003). Further evidence that MTs are involved in controlling root hair growth direction comes from the temperature-sensitive *mor1* (MT organization 1) mutants (Whittington et al., 2001).

Recent in vivo studies have provided new insights into MT dynamics in plant cells. Sieberer et al. (2002) showed that in vivo MT configurations during root hair development obtained with the green fluorescent protein (GFP)-MT-binding domain (MBD) fusion protein were similar to immuno-labeled fixed whole-mount samples. Two different populations of MTs were reported in *Medicago truncatula* (Sieberer et al., 2002). The cortical MTs (CMTs) are present in all developmental stages, and the endoplasmic MTs (EMTs) are present only in growing root hairs. Until now, EMTs have been reported only for legume root hairs and not in other species (Arabidopsis; Galway et al., 1997; Sieberer et al.,

2002). Despite the valuable information about MTs obtained from in vivo and inhibitor studies, a lot of questions remain unanswered about MT reorganization during root hair development. MTs change their configuration during root hair development (Geitmann and Emons, 2000; Sieberer et al., 2002), but it is not known how the transitional processes in MT reorganization occur. It still remains enigmatic how CMTs are formed in root hairs. Are they newly formed, or are they reorganized from existing CMTs? In addition, the reorganization of MTs during root hair outgrowth and tip growth is not understood.

In general, reorganization can occur by polymerization of new MTs, reorientation of intact MTs, or polymerization of existing MTs in a new direction (Kropf et al., 1998). Polymerization of new MTs requires the presence of nucleating sites. MT nucleation or formation is initiated at the γ-tubulin complexes located at the spindle pole body in yeast or at the centrosome in animal cells (for review, see Schiebel, 2000). In plant cells, the absence of organelles such as the centrosome has led to a lot of debate about the origin of MT nucleation sites (for review, see Schmit, 2002). It has been shown that the nuclear surface in higher plants has a centrosome-like activity (Mizuno, 1993; Stoppin et al., 1994). In addition, spontaneous and de novo assembly of nucleation sites may occur in the cell cortex, which was proved by semi-in vitro assays (Wasteneys et al., 1989), by studies of MT recovery after disassembly (Cleary and Hardham, 1987; Wasteneys and Williamson, 1989a), and by in vivo studies (Wasteneys et al., 1993; Erhardt et al., 2002; Chan et al., 2003; Shaw et al., 2003).

Another feature of MT dynamics adds to the complexity of MT reorganization. MTs are capable of rapid rearrangement by subunit exchange, which allows them to grow and shorten. These mechanisms have been thoroughly investigated in animal cells (for review, see Desai and Mitchinson, 1997) and to a lesser extent in plant cells (Zhang et al., 1990; Hush et al., 1994; Chan et al., 2003; Dhonukshe and Gadella, 2003; Shaw et al., 2003; Vos et al., 2004). Two mechanisms of subunit exchange are known. Treadmilling involves the addition of subunits to one (plus) end of an MT and loss of subunits from the opposite (minus) end. Dynamic instability is defined as a rapid switch between growth and shortening at the plus end of an MT (Cassimeris et al., 1988; Vorobjev et al., 1999). Mostly the minus end is less dynamic and oriented toward, or buried in, the MT organizing center-like structure. Recent experiments in BY-2 cells revealed the dynamics of MTs visualized with CYTOPLASMIC LINKER PROTEIN170-GFP (Dhonukshe and Gadella, 2003) or MBD-GFP (Vos et al., 2004). These studies showed that short periods of fast shortening are alternated with longer periods of slower growth. A hybrid MT-treadmilling mechanism, with dynamic instability at one end and slow depolymerization at the other end, has been demonstrated in cortical arrays of Arabidopsis epidermal cells (Shaw et al., 2003).

Transgenic Arabidopsis plants expressing a GFP-MBD of MT-associated protein-4 (MAP4) fusion protein (Marc et al., 1998) were used in this study to analyze the dynamic reorganizations of MTs during root hair development. This marker protein has proven to be very useful in previous cytoskeleton studies in Arabidopsis trichomes (Mathur and Chua, 2000), *M. truncatula* root hairs (Sieberer et al., 2002), and BY-2 cells (Dhonukshe and Gadella, 2003). Previous studies on dynamic instability in plant cells were based on two-dimensional (2-D; x, y) imaging methods where data are collected only from restricted regions in focus (Dhonukshe and Gadella, 2003; Shaw et al., 2003). As root hairs are often not lying completely parallel to the focal plane, 2-D imaging (x, y) would reveal only part of the MT organization in root hairs. Furthermore, 2-D scanning can lead to incorrect conclusions when MTs go out of focus. To have a complete view of MT dynamics in growing and full-grown root hairs, repeated three-dimensional (3-D) images (x, y, z, t) were taken over time (every minute). However, at some stages in development dynamics seemed so fast that the MT configuration was completely altered after 1 min. Therefore, additional fast-repeated 2-D scanning (x, y, t; a frame every second) with increased focal depth was performed at those stages. This study in Arabidopsis demonstrated that at the onset of root hair outgrowth MTs were reorganized, and during outgrowth new MTs are formed from distinct initiation sites. During root hair tip growth two populations of MTs could be distinguished. A new visualization method reveals prominent four-dimensional (4-D) data of MT polarity in mature root hairs. Finally, analysis of shortening events suggests turnover of subunits after apparent contact with neighboring CMTs. A model is discussed in which these shortening events play a role in a mechanism for CMT alignment.

RESULTS

To allow direct in vivo observations of MTs, transgenic plants stably expressing GFP-MBD of MAP4 were used (Marc et al., 1998). Arabidopsis plants carrying this construct were phenotypically normal and displayed normal root hair formation. As the root and the surrounding medium were transferred as a whole to the small-growth chamber suitable for microscopy, the root hairs continued to grow for several hours during imaging. The mean root hair growth rate during imaging was approximately 1 μm/min. This is in agreement with data from literature (Dolan et al., 1994) and suggests that root hair development was not affected by imaging.

MTs Reorganize and Apparent Initiation Sites Are Formed during Bulge Development

The cortical arrays in elongating epidermal cells formed helical arrays in which the MTs were oriented

transversely or at a slightly oblique angle (60–90° to the long axis of the cell). At the onset of root hair outgrowth, the MTs in the trichoblasts reorganized, whereas the MTs in atrichoblasts stayed in transverse arrays (Fig. 1, A and B). In the apical region of the trichoblast (near the bulge) the MTs disorganized (Fig. 1, A and B). This was also observed in lettuce by Takahashi et al. (2003a). At the onset of tip growth a smooth region appeared in the tip, which is known to contain vesicles (Galway et al., 1997). In the cortical region and apical cytoplasm of the outgrowing root hair, several discrete spots were observed with short-radiating MTs (white arrowheads and arrows, respectively, in Fig. 1D). To follow the dynamics of these structures over time, repeated 2-D sections (x, y, t) were taken. Supplemental Movie 1 focuses on the endoplasmic region and shows that the spots and the short MTs were very dynamic and moved simultaneously. Occasionally, MTs stayed in focus and as a result the elongation of MTs extending from the dense spots could be followed (black arrowhead in Fig. 1D; Supplemental Movie 1). Supplemental Movie 2 focuses on the (sub)-cortical region and illustrates the initiation and elongation of an MT. These observations suggest that the discrete spots are MT initiation sites.

Distinct Configuration Patterns of CMTs Versus EMTs in Elongating Root Hairs

MT configuration was followed in 4-D (x, y, z, t) during root hair expansion over long time periods. The 3-D time series images (x, y, z, t) were reduced to movies by projecting the maximum fluorescence of the confocal-optical sections for each time step to a 2-D image. In the cortical region an array with a high density of CMTs was observed (Fig. 2A; Supplemental Movies 3 and 4) similar to previous immunofluorescence studies (Lloyd et al., 1987; Geitmann and Emons, 2000). In addition to this cortical array, EMTs were observed in the cytoplasm of the root hair (Figs. 2, B–G, and 3). EMTs were previously demonstrated in legumes, but not in Arabidopsis. During early expansion EMTs accumulated in the cytoplasm (Fig. 2, K and L) and during late-growth stage bundles were formed in the cytoplasm (Fig. 2, N–P). During early root hair growth and before nuclear migration, EMTs extended between the subapical region of the tip and the
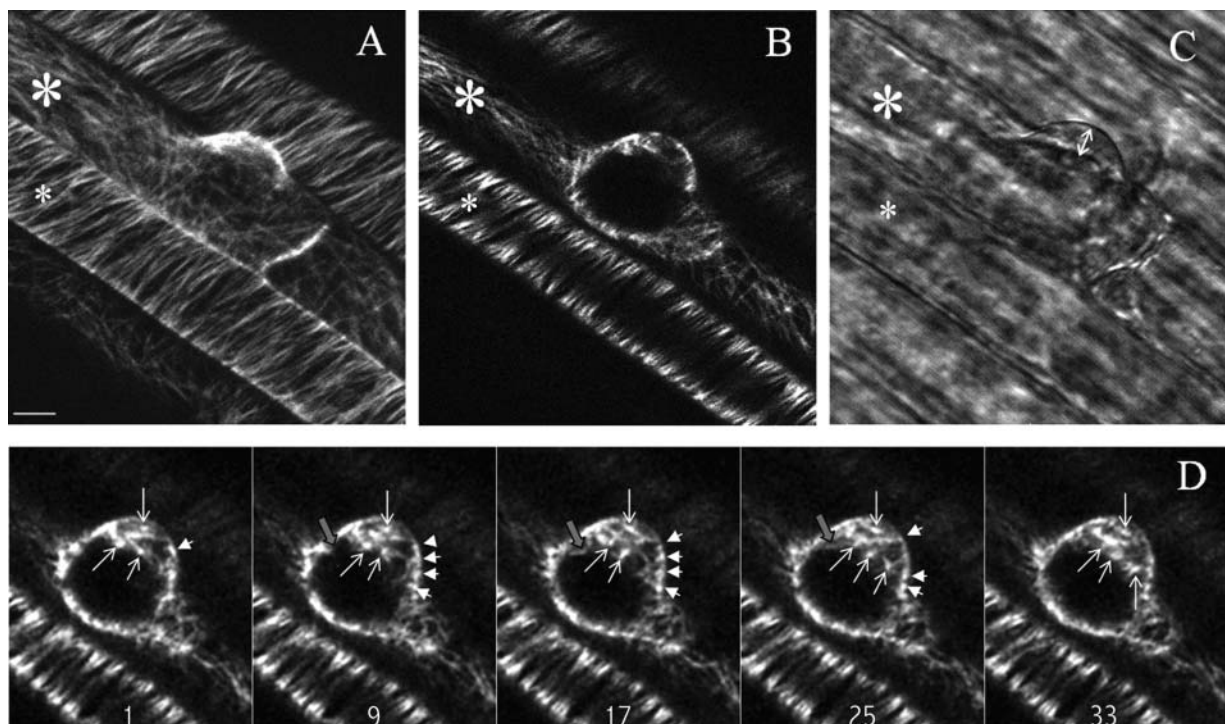

Figure 1. MT organization during bulge formation visualized with GFP-MBD of MAP4 and imaged with a confocal laser scanning microscope by 3-D sampling (x, y, z; A–C) and repeated 2-D sampling (x, y, t; D). A, Maximal projection of 25 optical sections at 1-μm (z) intervals of MTs in a bulge. The small asterisk indicates an atrichoblast; the large asterisk indicates a trichoblast. B, Single optical section at the endoplasmic region in the middle of the outgrowing root hair. C, Transmission image; double arrow indicates the vesicle-rich region of the outgrowing root hair. D, Time sequence showing the dynamics of apparent initiation sites. Five representative single-optical sections are shown from a series of 40 images taken at 1-s intervals (Supplemental Movie 1). The numbers indicate the time in seconds. The pointed arrows indicate the endoplasmic-apparent initiation sites, the arrowheads indicate the cortical-apparent initiation sites, and the gray-blocked arrow shows the growth of a single MT. Scale bar = 10 μm.
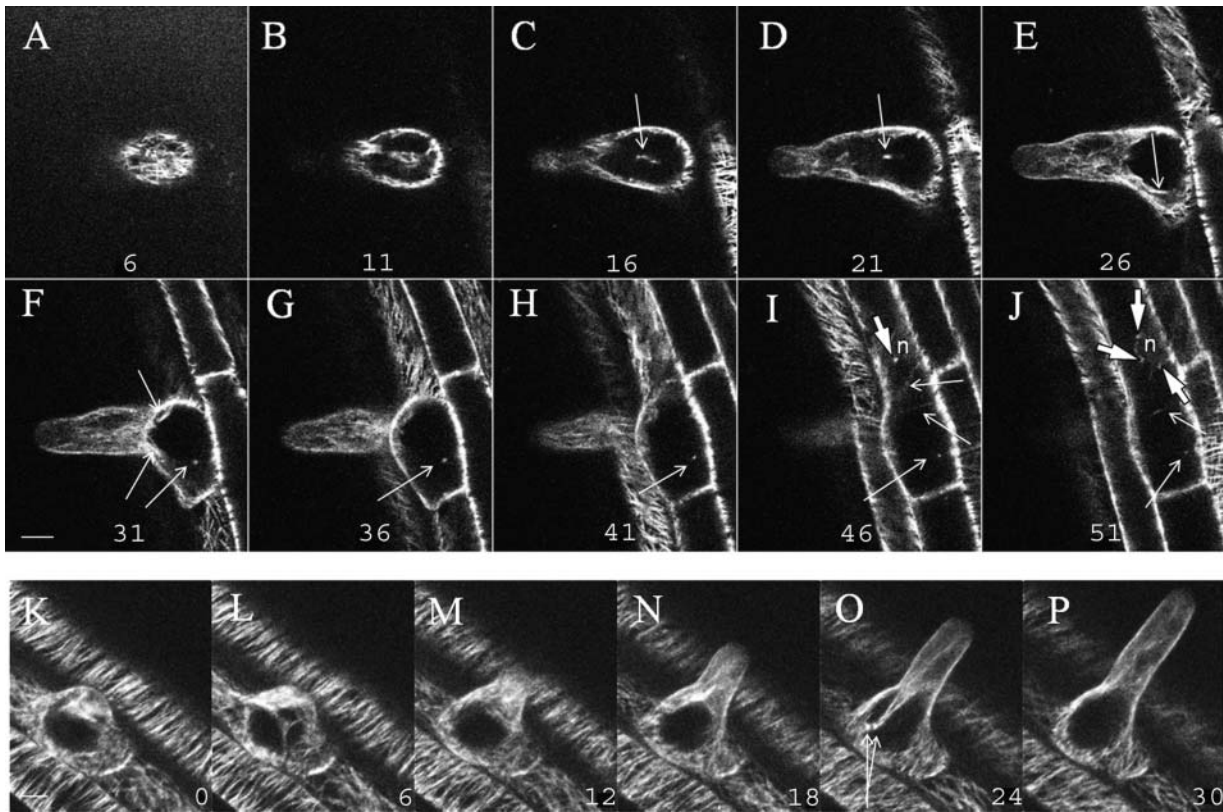
Figure 2. MT organization in a growing root hair visualized with a confocal laser scanning microscope in 3-D (x, y, z) and 4-D (x, y, z, t). The root hair is in an early stage of growth and the nucleus is not yet migrated into the tube. A–J, A series of 10 optical sections (x, y) with a separating distance of 2.5 μm. A, Optical section at the cortical region; E, optical section at the endoplasmic region. Arrowheads in I and J indicate the spots localized at the nuclear membrane, and arrows in C to J indicate cross sections of EMTs extending between the nucleus (n) and the tip or between the base and the tip of the root hair. Due to orientation of the cell and the EMTs, each optical section shows partial EMTs or cross sections of the EMTs. K to P, Six representative images from repeated 3-D scanning (x, y, z, t) over a period of 30 min. The numbers indicate the time in min. The images are represented as maximal projections of the four median-optical sections (x, y, z) with a separating distance of 1 μm in the endoplasmic region. The root hair was growing at a velocity of 1.4 μm/min. In O apparent initiation sites at the base of the root hair are indicated by arrows. Scale bar = 10 μm.

nucleus and occasionally between the base of the root hair and the nucleus (Fig. 2, C–J). Dense spots were localized at the surface of the nucleus (still in the main body of the cell), and MTs extended between these sites and the endoplasmic bundles (Fig. 2, I and J; Supplemental Movie 4). In the corresponding time series movie, spots seem to move along existing MTs (data not shown).

During further expansion of the root hair, the nucleus migrated into the tube and positioned at a more-or-less constant distance from the tip (Ketelaar et al., 2002). Figure 3A shows the situation after the nucleus has migrated into the root hair. Thick bundles of EMTs extended between the tip and the nucleus and formed an array around the nucleus. The cross section through the nucleus in Figure 3B clearly shows that the fluorescence was present at the edge of the nucleus and was most intense at the ends toward the tip and the base of the root hair. The EMT bundles branched in the tip and seemed to extend toward the CMTs in the subapical region. In highly vacuolated regions of the root hairs,

the EMTs were localized close to the cortex as the endoplasm was reduced to a thin layer between the vacuole and the plasma membrane. In this study, the EMT bundles at the subcortex were still clearly distinguishable from the CMT array but sometimes difficult to represent in a single projection. Supplemental Movie 5 shows the dynamics in the core-central sections and at a more upper level (including part of the CMTs). The EMTs are very dynamic and continuously change their orientation and configuration. Possibly these movements are related to the reorganizations of the cytoplasmic strands. Close to the bundles, individual fluorescent spots could be distinguished with short MTs radiating from these spots. The spots are clearly visible in the subcortex (lower part of Fig. 4A) and in the endoplasm (Fig. 4B; Supplemental Movie 6). MTs extending from the nucleus toward the cortex are indicated by arrows in Figure 4C. The elongation and reorientation of single MTs were imaged by repeated 2-D images (x, y, t) with increased focal depth taken every second (Supplemental Movie 6).
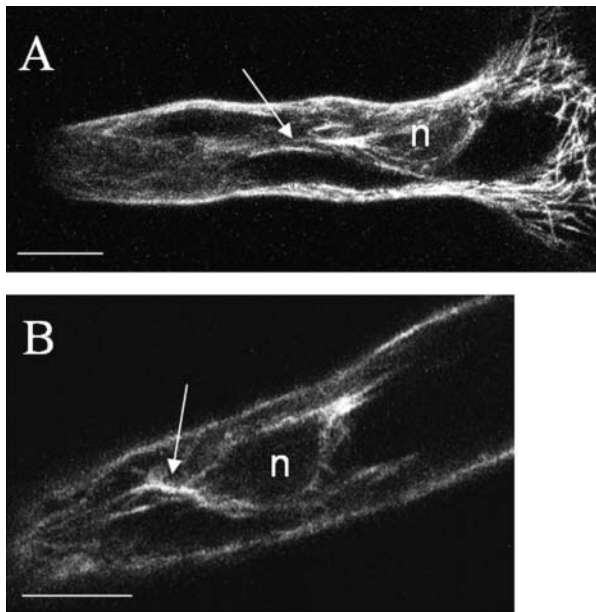
Figure 3. Configuration of EMTs around the nucleus (n) in late-stage-growing root hairs visualized with a confocal laser scanning microscope. A, Maximal projection of four median-optical sections at a separating distance of 1 μm; arrow indicates EMT bundle extending toward the tip. B, Single optical section through the nucleus. EMT fluorescence is present at the edge of the nucleus and is most intense at the ends toward the tip and the base of the root hair (arrow). Both root hair tips are oriented to the left. Scale bar = 10 μm.

these reorganizations coincide with MT rearrangements. One of the features visible during growth arrest was that the vesicle-rich region narrowed and finally completely disappeared in full-grown root hairs (compare Fig. 5, A, E, and I). The cytoplasmic streaming changed from reverse-fountain streaming to circular streaming, as described earlier by Miller et al. (1997) and Sieberer and Emons (2000). At that time the nucleus left its position close to the tip and kept on moving back and forth in the mature root hair (Chytilova et al., 2000; Ketelaar et al., 2002; Van Bruaene et al., 2003).

There are three major configuration differences between growing and full-grown root hairs. First, and most obviously, there are fewer CMTs in full-grown root hairs compared to elongating root hairs (Fig. 5, B versus J). The growing root hairs had a high-density array of CMTs. In full-grown root hairs, CMTs had a longitudinal or helical organization (for review, see Geitmann and Emons, 2000); only very few MTs were transversely oriented. Second, the MTs in elongating root hairs didn't reach the very tip, whereas some MTs reached the very tip in growth-arresting root hairs and could even curve in the tip of mature root hairs (Fig. 5, B, F, and J, respectively). Third, the EMTs disappeared during growth arrest and there were no MTs extending between the nucleus and the tip in full-grown root hairs (compare Fig. 5, C, G, and K). Occasionally, short MTs were observed close to the nucleus in full-grown root hairs.

The Organization Pattern of MTs in Elongating Root Hairs Is Different from the Pattern in Full-Grown Root Hairs

Since cytological structures rearrange during growth arrest, it was interesting to investigate whether

MTs Reassemble after Complete Depolymerization with Oryzalin

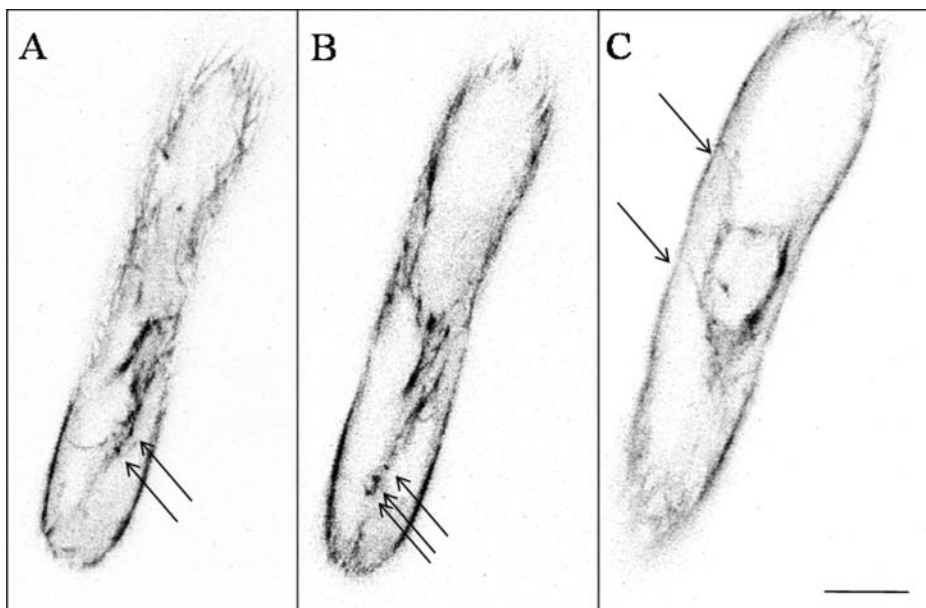To determine whether MTs can reassemble independently from the interior organizing sites such as

Figure 4. Configuration of EMTs in late-stage-growing root hairs. Images are shown using an inverted grayscale to enhance the details. A, A representative image is shown out of a series of single optical sections taken every sec (x, y, t) with increased pinhole of 3 airy disc units. The complete sequences of 30 s are available as Supplemental Material (Supplemental Movie 6). The root hair is tilted and the image grazes only the cortex at the upper half of the image. The lower half shows the subcortical region; spots are indicated by arrows. B, Single optical section at the center of the root hair showing EMT bundles and spots (arrows). C, Optical section through the nucleus, single EMTs extend from the nucleus toward the cortical region (arrows). Root tip is oriented downwards. Scale bar = 10 μm.
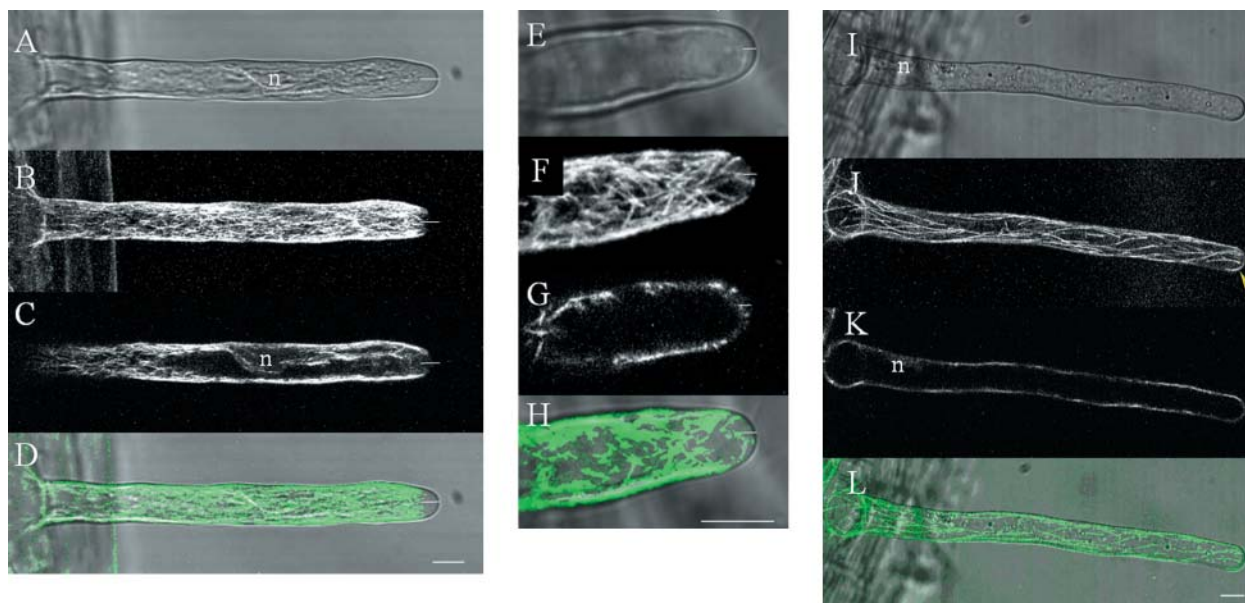
Figure 5. Comparison of MT organization between late-stage-growing (A–D), growth-arresting (E–H), and full-grown (I–L) root hairs. Transmission images show the cytoarchitecture (A, E, and I); maximal projections of four upper-optical sections (x, y, z) show the CMTs (B, F, and J); maximal projections of four median-optical sections (x, y, z) show the EMTs (C, G, and K). Combination of the CMTs and transmission data show the relation between the cytoarchitecture and the CMT configuration at the root hair tip (CMTs in green; transmission in gray; D, H, and L). The nucleus is indicated by n, short white lines indicate the vesicle-rich region, and the yellow arrow indicates an MT curving in the root hair tip. Scale bars = 10 μm.

the nuclear surface, root hairs were depleted of MTs by the depolymerizing drug oryzalin. The MTs in the root hair and its cell body were completely depolymerized after a 10-min treatment with 1 μM oryzalin but not in the neighboring epidermal cells (Fig. 6A). It is nearly impossible to visualize the MT configurations within a single root hair before and after drug application because manipulation alters positioning of the root hair and observation has to start directly after treatment. However, all root hairs had normal MT configurations before treatment. Only 10 min after washing out the oryzalin drug, the first signs of recovery were observed. Single dense spots appeared at the cortex in the epidermal cell and in the root hair tube (Fig. 6A; Supplemental Movie 7). In the following minutes MT clusters were formed in the (sub)-cortex (Fig. 6A) and in the endoplasm (Fig. 6B) at the places where the dense spots first appeared. Some clusters were very similar to the branching clusters observed by Wasteneys and Williamson (1989a); others had a thick appearance, suggesting bundling. At a later stage the MT organization became less clustered and resembled more the original configuration. After a 20-min recovery there were still fewer MTs than in the original configuration. These results demonstrate that MTs can nucleate at sites different from the organizing centers at the nuclear surface. In addition the results confirm previous results showing that MTs are first formed in a disordered configuration and reorder at a later stage (Wasteneys and Williamson, 1989a, 1989b; Baluška et al., 1992).

Dynamic Instability of MTs Revealed with Difference Imaging

In the nondrug-treated cells a method was developed to better visualize the CMT dynamics. Each frame of the movie is compared with the following frame by combining the pair into a single color image. Each frame forms the red channel when it is the first of a pair (Fig. 7A) and the green channel when it is the second of a pair (Fig. 7B). The resulting color movie aids visualization of changes in the MT cytoskeleton over time (Fig. 7C). Fluorescence present only in the first image of each pair appears red; fluorescence present only in the second image of each pair appears green; fluorescence levels that remain constant from frame to frame will combine the red and green channels to appear yellow in the difference image (Fig. 7, C and D). The MTs of fixed cells lacking dynamics will appear completely yellow. Transmission images taken together with the fluorescence images served as control for possible specimen drift.

In elongating root hairs few MTs remained in the same position between two sequential time points at 1-min intervals. This reorientation may be caused by MT translocation or turnover. The fast reorientation together with the high-MT density makes it difficult to distinguish between these two possibilities. The intensity profiles along the root hair of those pixels in Figure 7C that are exclusively green or exclusively red are plotted in Figure 7E and give information about the net growth and shortening. The green peak close to the
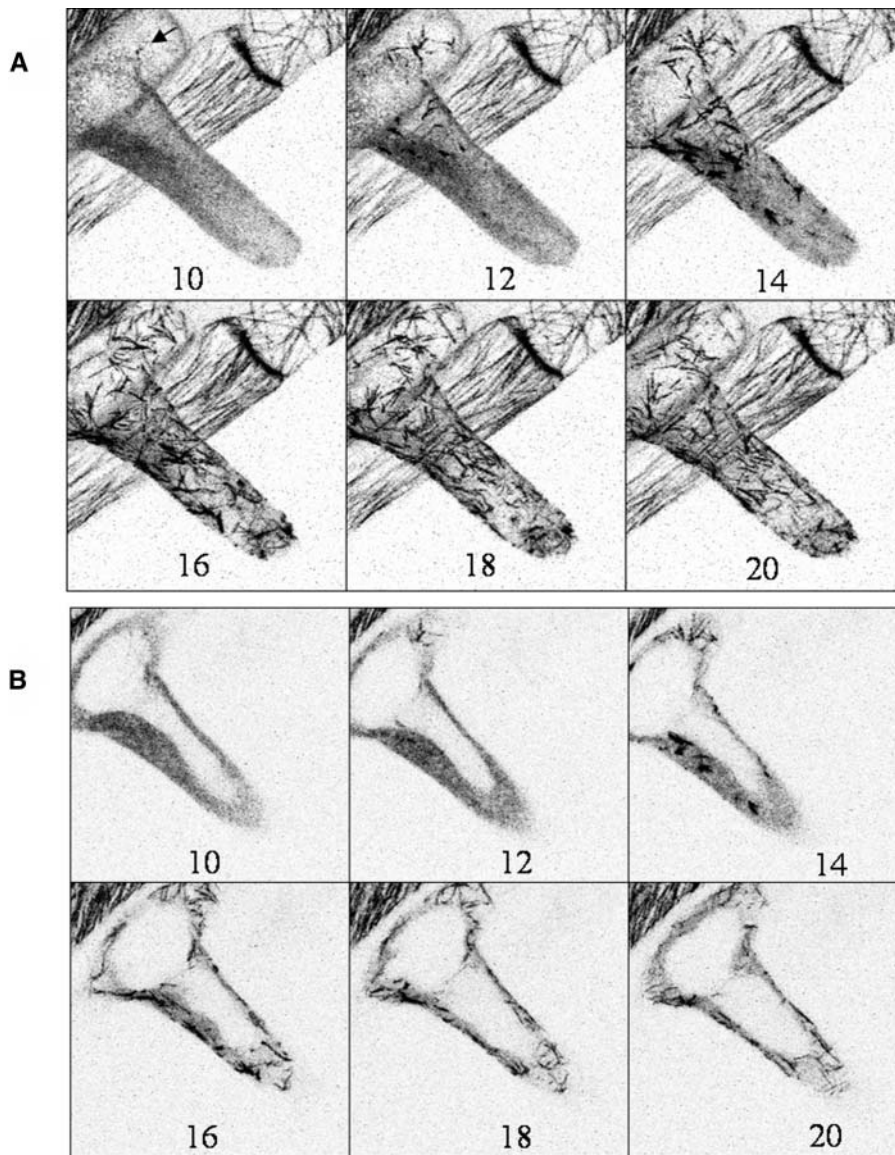
Figure 6. Visualization of MT recovery in an early stage-growing root hair following a 10-min treatment with the MT depolymerizing drug oryzalin (1 μM). The inverted grayscale image is shown to enhance the details. The numbers indicate the minutes after washing out oryzalin. A, Six images out of a time sequence of optical sections taken every minute (x, y, z, t). Numbers indicate time in minutes. The images represent maximal projections of 20 optical sections at a separating distance of 1 μm. B, Six images of the same time sequence as A, but maximal projections are restricted to the three median-optical sections through the endoplasmic region. The nucleus had not yet migrated in the root hair tube. Scale bar = 10 μm.

vesicle-rich region indicates formation of new MTs during root hair growth. This increase in fluorescence indicates either de novo MT formation in the new part of the root hair or extension of MTs from the old region into the new. On the other hand the red peak, representing MTs in the first frame that are absent in the second, indicates that MT density is reduced behind the region of newly appearing MTs, represented by the green peak. This suggests that most MTs that were formed close to the vesicle-rich region translocated toward the tip or depolymerized during the next minute.

It was not possible to directly make the distinction between putative-bundled CMTs and individual CMTs due to the limited resolving power of the microscope. However, in full-grown root hairs several observations support the idea that dynamics of single CMTs were observed. First, CMTs were never ob-

served to move laterally or merge to another CMT so that they could no longer be individually resolved; second, newly formed CMTs and existing MTs showed equal intensity; and finally the dynamic-instability data (see below) indicated that the CMTs were one continuous unit as complete shortening was observed. Therefore, as there was no indication that bundled CMTs occurred in full-grown root hairs, in the subsequent results the observed CMTs will be regarded as single CMTs.

The visualization method also proved very useful to analyze changes of the CMTs in full-grown root hairs. Different characteristics of the individual CMTs were revealed. In contrast to the CMTs in growing root hairs, most of the CMTs in full-grown root hairs are colored in yellow (Fig. 7H). There are no green or red changes along the yellow MTs, supporting the idea that the observed MTs in full-grown root hairs are
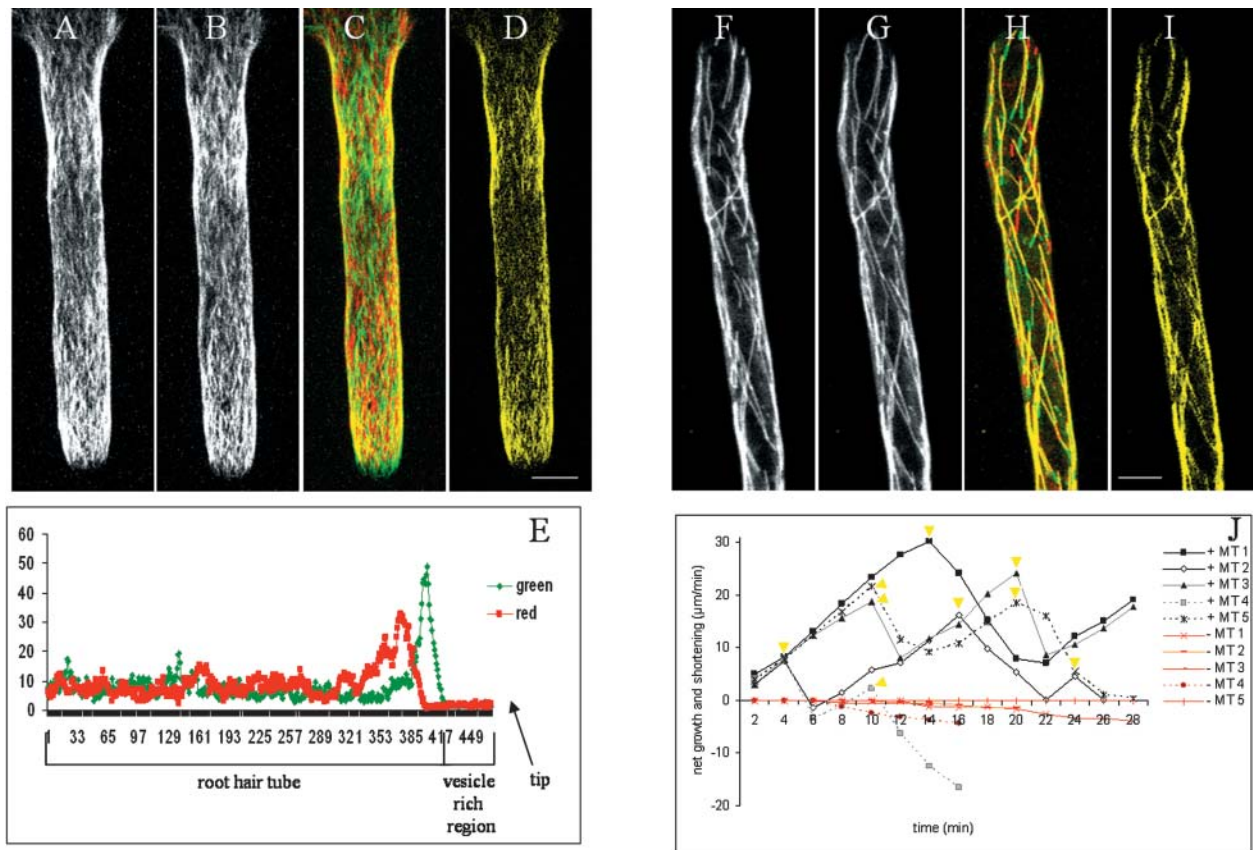
Figure 7. CMT dynamics in late-stage-growing (A–E) and full-grown (F–J) root hairs. Configuration of CMTs in growing and full-grown root hair represented as maximal projection of 20 optical sections (separating distance 1 μm) at 0 min (A and F) and at 1 min (B and G). Difference images of two time points (C and H), the images at 0 min (A and F) from the red channel, and images at 1 min (B and G) from the green channel. CMTs that did not change in position or length appear yellow (see also D and I). Intensity profile of red and green (not yellow) pixels along the root hair axis (length = 470 pixels; E). Root hair tip is not shown in F to I but oriented downwards. Life history plots show individual dynamics of CMT plus and minus ends. The yellow triangles indicate the time points where an apparent contact was detected. The deviation in orientation of the growth direction in respect to the previous growth direction for the different MTs: MT1, 8°; MT2, 7° and −2°; MT3, 5° and −3°; MT4, −7° and 11°; and MT5, 2°. Negative values indicate counter clockwise deviations (J). Scale bars = 10 μm.

single MTs (Supplemental Movie 9). This is in contrast with the green and red portions appearing along the yellow MTs in the transverse arrays of nonroot hair epidermal cells (data not shown), which suggests dynamics of multiple MTs lying along each other. In full-grown root hairs no MT displacement was observed in the z-direction (Fig. 8A; MT remains yellow); green and red portions were observed only at the MT ends. In addition, the majority of CMTs showed no lateral movements over time (Fig. 8, B and C). These two observations suggest that the CMTs were fixed to the cortex, corresponding to the observations of Shaw et al. (2003). However, some newly formed MTs showed clear lateral movement as indicated in Figure 8D. Vertical cross sections demonstrate that the MT was subcortical. Newly formed MTs were probably not yet fixed to the cortical region.

Another important feature that could be directly determined from the difference images is the amount of growth (green) and shortening (red) at the MT ends (Fig. 7, F–I). The dynamics of both MT ends of five

CMTs are depicted as MT life history plots in Figure 7J. The plots demonstrate that the growth rate is lower than the shortening rate, corresponding with the data of Dhonukshe and Gadella (2003) and Vos et al. (2004). It should be noted that the plots may represent an underestimation of the real situation, especially at the transition points where growth switches to shortening and vice versa. In contrast to these dynamic (plus) ends, the opposite minus ends were characterized with slow (72%) or no (28%; total $n = 146$) shortening (Fig. 7J). Only limited examples of breakage in CMTs were recorded (less than 2%).

Detailed analysis of the behavior of 174 CMTs in 10 different full-grown root hairs revealed that the majority of CMT plus ends were oriented toward the root hair tip (82% ± 9%). Only 11% ± 6% of the plus ends were oriented toward the base and 7% ± 5% were transversely oriented. The difference image Figure 7H showing shortening in red and growth in green revealed that fast shortening of MTs occurred over the whole length of the full-grown root hair. Shorten-
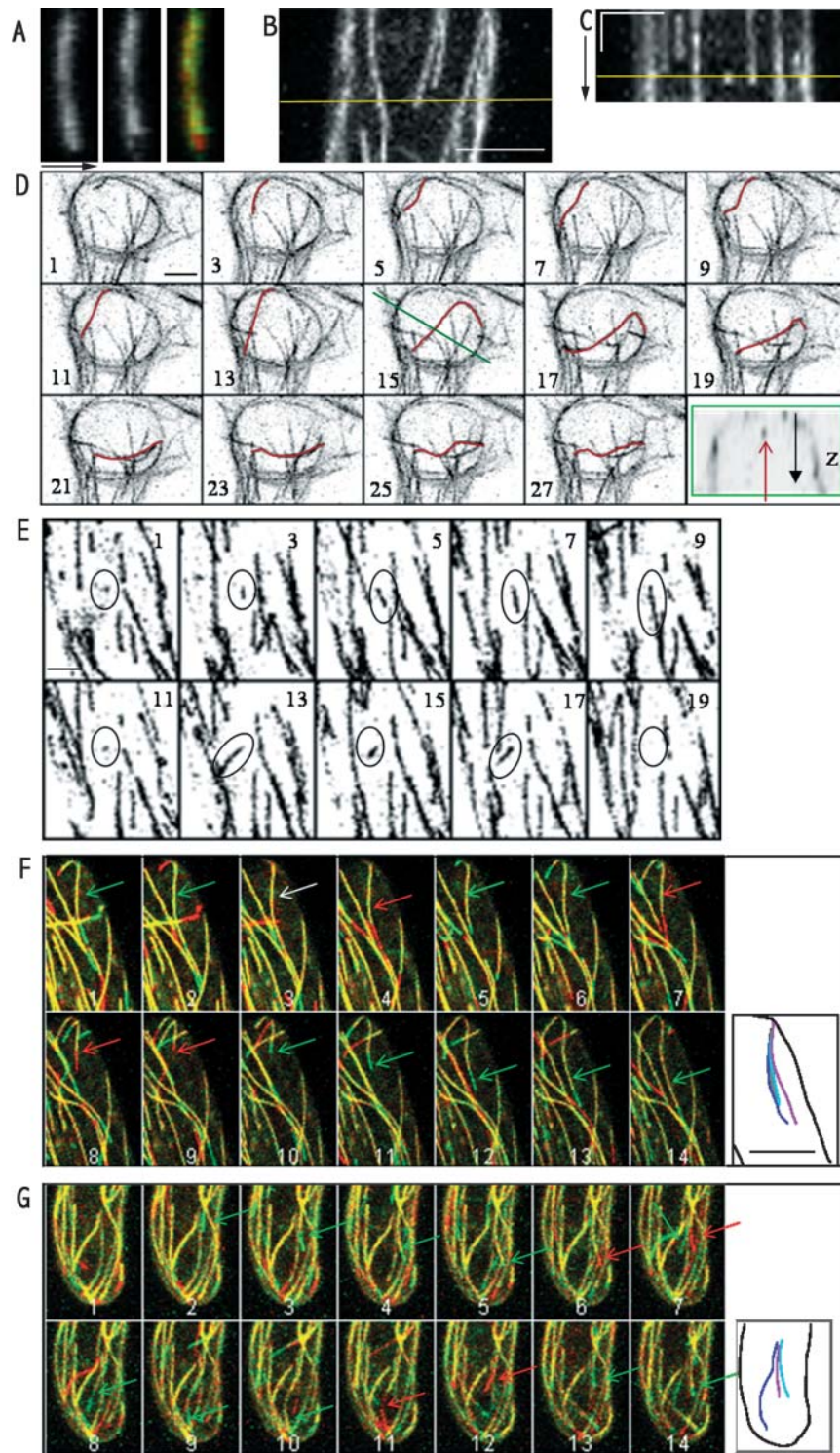
Figure 8. CMT position and dynamics in full-grown root hairs. A, Vertical positioning of an MT over time; transects (x, z) through z-depth of an MT at two different time points (left section = 0 min, middle section = 20 min). The difference image (right section) in lower section shows that the MT did not move in the z-direction. Arrow indicates the z-direction. Height and width of image box is 6 and 14 μm, respectively. B, Maximal projection of (x, y, z) stack at one time point. Scale bar = 8 μm. C, Kymograph of a transect (yellow line in B) through the time sequence of maximal projections. Straight lines indicate no lateral movement of the MTs during the 30-min experiment. Vertical bar = 10 min, horizontal bar = 5 μm. Yellow line indicates position of maximal projection in B. D, Sequence of 14 images from repeated 3-D optical sections over time (x, y, z, t). Numbers indicate the time in minutes. The inverted-grayscale images are maximal projections of 20 optical sections with a separating distance of 1 μm taken at the base of the root hair. Newly formed MT shows lateral movement in the time sequence (MT colored in red). The green box in

Table I. *Association of the CMT-shortening events with apparent contacts of a CMT plus end with another CMT*

Apparent contacts of a CMT plus end with another CMT may result in shortening or crossing. Shortening in seven cells associated or not associated with apparent contacts. Numbers correspond with number of events; the relative percentages are mentioned in the text.

	Apparent Contacts	Shortenings	Crossings
	100	100	–
	38	–	38 (17/38 with transverse CMTs)
	–	25	–
Totals	138	125	38

ing events at MT plus ends could result in complete depolymerization of CMTs (MT4 in Fig. 7J). MTs that did not show depolymerization at the minus end before complete depolymerization of the plus end recovered in the next minute from the original initiation site. On the other hand, MTs that showed slow depolymerization at the minus end did not recover after complete depolymerization (MT4 in Fig. 7J). This suggests that the MT initiation site is inactivated after minus-end depolymerization.

Dynamic Instability of CMT Plus Ends after Apparent Contact with Other CMTs

Inspection of the movies (e.g. Fig. 8, F and G; Supplemental Movie 9) revealed another striking feature. When a CMT plus end apparently contacted another CMT, the CMT partly or completely depolymerized. Repeated 2-D (x, y, t) imaging of restricted well-focused regions showed that shortening after apparent contact occurs after a pause of 30 to 60 s with no length change. To better quantify the significance of this observation the number of CMT shortening events and apparent contacts of a CMT plus end with another CMT were counted in seven cells (Table I). The data clearly show that most shortening events occurred after the leading plus end encoun-

tered another CMT (80% ± 9%). Only 20% ± 10% of the shortenings occurred without apparent contact. Apparent contacts of plus ends with other CMTs could also result in crossings without shortening, but this occurred at a much lower frequency (27.5% ± 5%). In addition approximately 50% of this type of apparent contact occurred with transversely oriented CMTs (Table I), which were markedly shorter in length than the other more longitudinally oriented MTs. The data in Table I represent only the dynamic events during imaging. Only those crossing events that occurred during imaging were counted, as also the previous apparent contacts could not be taken into account. As the time gap between the images is 1 min, the growth or shortening within this period cannot be visualized. Due to this limited-time resolution, the dynamics of the MTs may be underestimated; e.g. it is possible that the growth and subsequent rapid shortening taking place between two time points is seen as a net shortening. In this respect, the number of events within the class of shortenings without apparent contact might be overestimated. However, as there is a pause of 30 to 60 s with no change in length after encountering another MT, the chance to observe an MT in an apparent contact state is high, and the chance that growth, apparent contact with pause, and subsequent rapid shortening occurs completely within the timeframe of 1 min (observed as a shortening without an apparent contact) can be expected to be low.

Interestingly, those CMTs that recovered after shortening ($n = 64$) all grew back in a slightly different direction. In the extra sections of Figure 8, F and G two examples are depicted where an MT in this way showed three subsequent different orientations during one movie of 30 min. The apparent contacts followed by shortening are indicated by yellow triangles in Figure 7J, and the deviation in growth direction ranged from 2° to 11° (see figure legend Fig. 7J). These observations suggest that the reorientation of a CMT after apparent contact is part of a mechanism for MT alignment. To test this hypothesis, the frequencies of shortening events were observed in root hairs with

Figure 8. (*Continued.*) the extra section reveals the subcortical position of the MT in question and represents a (x, z) cross section taken through the optical sections at time point 15 min (position indicated by the green line in 15-min image). The red arrow shows the position of the single MT colored in red. The black arrow is the axis of increasing z. Scale bar = 5 μm. E, Formation of a new CMT. Sequence of 10 images from repeated 3-D optical sections over time (x, y, z, t) taken every minute. The images are maximal projections of the four upper-optical sections (with a separating distance of 1 μm) taken at the level of the cortex of the root hair. The ellipse indicates a single CMT. Initial growth is followed by complete shortening. Subsequent growth from the same site results in growth in a slightly different direction. This process is repeated several times over 20 min. Scale bar = 5 μm. F, Dynamic instability of CMTs at the base of the root hair. The images are the result of maximal projections of four upper-optical sections at a separating distance of 1 μm repeated over time (every 2 min). Numbers indicate number of section. Dynamics is illustrated by the green (growth)/ red (shortening) difference image. For detailed information concerning this technique, see results section. An individual CMT is indicated by an arrow. The green, red, and white color of the arrow indicates growth, shortening, and pause, respectively. Extra section shows reorientation of CMT after a shortening event and subsequent growth; light-blue line corresponds with time point 3, dark blue with time point 6, and magenta with time point 14. Scale bar = 10 μm. G, Dynamic instability at the root hair tip represented in the way as explained in F. Note that section G7 shows two arrows indicating shortening and subsequent growth in a different direction of the same CMT. Light-blue line in extra section shows CMT position at time point 5, dark blue at time point 9, and magenta at time point 14. All root hairs tips are oriented downwards.

Table II. *Configuration of CMTs related to the density of CMTs and number of shortening events in three different mature root hairs*

CMT density is the mean number of CMTs measured on different cross sections (indicated by *n*) through the root hair regularly spaced along root hair axis; no. shortening events is the mean number of shortening MTs (labeled red) in the root hair tube measured every 2 min in a movie over a period of 30 min (measuring no. of shortening events as count of shortening MTs only in alternate frames ensures that they are not double counted as the events don't persist long enough); length is the mean length of all CMTs in μm; angle is the angle measured between the axis of CMT (plus/minus end) and the root hair axis in degrees. Length and angle were measured in one typical frame. For every parameter the SEM was calculated, the number of repeats being indicated between brackets.

Root Hair	CMT Density	No. Shortening Events	Length	Angle
			μm	$^\circ$
1	3.29 ± 1.81 (*n* = 20)	7.43 ± 2.73 (*n* = 15)	29.22 ± 2.94 (*n* = 15)	9 ± 1.81 (*n* = 15)
2	3.90 ± 1.97 (*n* = 31)	7.71 ± 2.78 (*n* = 15)	16.65 ± 0.60 (*n* = 23)	14 ± 1.46 (*n* = 23)
3	5.38 ± 2.32 (*n* = 40)	23.0 ± 4.80 (*n* = 15)	6.77 ± 0.22 (*n* = 40)	25 ± 3.00 (*n* = 40)

different densities of CMTs. In a root hair with fewer CMTs (Table II, root hairs 1 and 2), significantly fewer shortening events occurred over time than in root hairs with more CMTs (root hair 3). One would expect a shorter CMT length if more shortening events occur. Indeed, the CMT lengths were significantly shorter in root hair 3 compared to root hairs 1 and 2 (Table II). Finally, the CMTs in root hairs 1 and 2 are more uniformly aligned than in root hair 3 (Table II). Presumably, root hair 3 was more recently arrested in growth, showing more CMTs but less well aligned CMTs. Together with the fact that CMTs grew in a slightly different direction after shortening (Fig. 8, F and G) and the fact that some CMTs completely depolymerized after apparent contact, this process may finally result in fewer, longer, and better aligned CMTs (root hairs 1 and 2). Data modeling for the different parameters will be performed in the future to investigate if this correlation is real.

DISCUSSION

MT Reorganization Precedes Change of Growth Direction

At the onset of root hair outgrowth MTs disorganize in Arabidopsis in trichoblasts, in contrast to the transverse arrays in the atrichoblasts (Fig. 1A). Similar results have been reported for maize and lettuce (Baluška et al., 2000; Takahashi et al., 2003a), except for *M. truncatula*, where the CMT arrays are still transversely organized at the onset of polar outgrowth (Sieberer et al., 2002). In lettuce it was demonstrated that MT disorganization is necessary for bulge formation and can be induced by acidification or treatment with MT-depolymerizing drugs (Takahashi et al., 2003a). Recent observations demonstrated that hormones such as ethylene and auxin might be involved in CMT randomization (Takahashi et al., 2003b). In addition, reduced α-tubulin gene expression in Arabidopsis causes formation of multiple and ectopic root hairs (Bao et al., 2001). How MT reorganization is exactly coupled to root hair formation needs to be further analyzed.

Formation of New MTs during Root Hair Development

Reorganization of MTs during root hair development is in part the result of polymerization of new MTs. MT initiation sites were observed as discrete spots with radiating MTs at the onset of root hair outgrowth and near the EMTs during root hair growth. MTs also initiate at the (sub)-cortex in full-grown root hairs, but the initiation sites are not distinct from the MTs. Due to the dense CMT array in growing root hairs it is impossible to see if there are discrete spots. MTs in the newly formed tip are continuously added during growth. If fluorescent spots indicate new initiation sites of MT formation, there is no evidence that new MTs are formed near the vesicle-rich region. Therefore, MTs in the region near the vesicle-rich region have to be extensions of MTs from the old region. At present there are different views about the origin of the CMTs. One model suggests that all MTs are nucleated at the nuclear membrane and then transported (overview in Lambert and Lloyd, 1994), whereas others claim that MTs originate at dispersed nucleation sites (Wasteneys and Williamson, 1989a; Wasteneys et al., 1993; Erhardt et al., 2002). Data in growing root hairs are consistent with dispersion of MT initiation complexes from the nuclear surface along existing EMTs (Wasteneys, 2002). The recovery experiment of reassembly of MTs after complete depolymerization in root hairs shows that MT-nucleating factors can be located at sites other than the nuclear surface during root hair outgrowth. The patterns of the recovered MTs after complete depolymerization by oryzalin (Fig. 6) closely resemble the branching clusters described earlier (Wasteneys and Williamson, 1989a, 1989b). The formation of these structures was explained by a model proposing that MT-initiating factors move along existing MT tracks and nucleate the assembly of new MTs at different angles from preexisting MTs (fractal tree model; Wasteneys, 2002). At steady state this mechanism might be present as well but too fast to visualize. It should be kept in mind that the nucleation after disassembly is not a natural process, as reassembly takes place under a biochemically abnormal condition such as high tubulin concentrations. Use of in vivo markers of MT nucleation, such

as AtSpc98p-GFP (a proposed MT organizing component; see Erhardt et al., 2002), might reveal more exactly where the MTs nucleate during root hair development.

EMTs Bundles Extend from Nucleus to Root Hair Tip in Growing Root Hairs

This in vivo study demonstrated EMTs for the first time, to our knowledge, in Arabidopsis root hairs. EMTs could not be demonstrated by immunofluorescence previously (Ketelaar et al., 2002). It is possible that the fixation procedure made the EMTs disappear, since EMTs disappear quickly during growth arrest (this study; Sieberer et al., 2002). Alternatively, it might be that the antitubulin antibodies do not recognize or reach the EMT structures. In highly vacuolated regions of the root hair the EMTs have a subcortical localization, and this might be the reason why the EMTs were overlooked in a previous ultrastructural study in Arabidopsis (Galway et al., 1997). Staining with antitubulin antibodies in *Vicia sativa* root hairs revealed endoplasmic, axial bundles (Lloyd et al., 1987), very similar to the EMTs observed in this study in Arabidopsis. In *M. truncatula* root hairs the EMTs form a dense array through the subapical-dense region between the tip and the nucleus, but no bundles were observed (Sieberer et al., 2002). This difference in MT organization can be explained by the difference in configuration of the subapical region. The tip nucleus distance is smaller in *M. truncatula* (30–40 μm) than in Arabidopsis (40–70 μm; compare Ketelaar et al., 2002, and Sieberer et al., 2002). In Arabidopsis, vacuolar compartments or precursors can accumulate in the region between the nucleus and the tip. This may reduce the subapical region, resulting in more bundled EMTs. The different EMT configuration in *M. truncatula* could be related to a specialized function in legumes to interact with rhizobia.

Before nuclear migration perinuclear EMTs in Arabidopsis growing root hairs extend from the nucleus toward the tip. During nuclear migration the perinuclear EMTs form a very tight array surrounding the nucleus and extend as bundles in the subapical region toward the tip. In *M. truncatula* root hairs EMTs are thought to configure the subapical region and to be necessary to keep the nucleus close to the root hair tip (Sieberer et al., 2002). EMTs are thought to play a role in the growth machinery of root hairs and to strongly influence the growth pattern (Bibikova et al., 1999; Weerasinghe et al., 2003). EMTs may be involved in the transport of new nucleation complexes from the nucleus to other places in the root hair. Different studies also give evidence that MTs may act as organizing elements to position the actin filaments (Tominaga et al., 1997; Justus et al., 2004). The dynamics of the EMTs may be related to the organization of the cytoplasmic strands, as the data suggest that the movements of the EMTs and cytoplasmic strands are correlated. In other cells, perinuclear MTs are observed only briefly as cells reenter interphase, probably because of their transient nature (Hasezawa et al., 2000). In contrast, perinuclear MTs are prominent in *fra2* mutants (Burk et al., 2001), probably because the severing of the perinuclear MTs is delayed in these mutants. The dense spots observed at the nuclear envelope in the *fra2* mutant look similar to those observed in growing root hairs.

Dynamic Instability of CMT Plus Ends after Apparent Contact with Other CMTs

CMT dynamics in full-grown root hairs was analyzed in detail using difference images. CMTs showed no lateral or z-direction movement, except if newly formed. Possibly, CMTs became anchored to the cortex by specific MAPs during maturation (for review, see Lloyd and Hussey, 2001; Hussey et al., 2002; Mayer and Jürgens, 2002; Wasteneys and Galway, 2003). The majority of the MTs showed dynamic instability at the plus end and slow depolymerization at the minus end. This process is called hybrid treadmilling and has recently been observed in plant cells (Shaw et al., 2003). There are no indications that CMTs are physically moving in the direction of the polymer, as there is no correlation between plus- and minus-end dynamics. However, experiments based on fluorescence photobleaching could not rule out this possibility, as recovery was too fast with the MDB-GFP marker (data not shown). This later result demonstrates that MDB-GFP is a reliable marker for MT dynamics, as this MAP decorates MTs very rapidly. The observation of slow depolymerization from the minus end suggests release of the MT from the initiation complex. This release can occur by dissolution of the MT initiation complex or through cleavage near the minus end by a katanin-like protein. Molecular candidates for severing activity have been recently discovered in Arabidopsis (Bichet et al., 2001; Burk et al., 2001; Webb et al., 2002) and the in vitro severing activity of AtKSS has been demonstrated (Stoppin-Mellet et al., 2002).

Quantitative results revealed that the plus ends of CMTs seemed to shorten due to other CMTs in their path (Table I). Shortening events mainly occurred (80%) when the plus end of one CMT encountered another CMT (Table I). Since two populations of CMTs were observed, those that appear to be anchored to the plasma membrane and those located at a slightly different level in the subcortex, this may explain the apparently different behavior following an apparent contact. If the CMTs are both anchored to the plasma membrane, then a contact is likely to be real. Otherwise the two CMTs are likely to just cross the line of sight at different levels. Transverse CMTs are likely to be positioned at a slightly different level in the cortex and cross with other CMTs rather than collide. Transverse MTs are shorter in length and might not yet be anchored to the cortex, which can explain their different positioning. The feature of shortening after contact is probably more obvious in plant cells than in animal

cells, as dense arrays of CMTs are confined to a thin cortical layer in plant cells.

One possible explanation for shortening after apparent contact is based on force in encountering an obstacle. There is evidence for this in vitro (Janson et al., 2003). Another possibility is that, after apparent contact, molecular interactions result in the activation of destabilizing factors and/or inactivation of stabilizing factors. Candidates for these interactions are a shortening-inducing kinesin of the kin-1 family (XKCM1 in Xenopus, Walczak et al., 1996; KMCM1 in mammalian cells, Kline-Smith and Walczak, 2002) and the stabilizing factor XMAP215. The N terminal of XMAP215 works antagonistically with XKCM1 by stabilizing MTs (Tournebize et al., 2000) and is homologous to the N-terminal domain of MOR1 in Arabidopsis (Whittington et al., 2001). *Mor1* mutants have disorganized CMTs at the restrictive temperature (Whittington et al., 2001). According to Hussey et al. (2002) the N-terminal repeat of MOR1 could bind directly to a destabilizing kinesin or compete with it for the MT-binding site. Future experiments may provide new insights into whether these molecular players are involved in the regulation of MT dynamics.

A New Mechanism for CMT Alignment in Full-Grown Root Hairs

It is clear that reorganization is a distinct process from initiation of the MTs, as MTs first appear as disorganized structures and order later (this study, Fig. 6; Wasteneys and Williamson, 1989b). Reorganization of existing MTs could occur by either of two mechanisms, translocation or turnover. Previous studies have known that factors such as light, hormones, electrical fields, calcium, pH, mechanical pressure, gravity, and wounding can elicit MT reorientations in transverse-cortical arrays (Cyr, 1994; Hush and Overall, 1996; Granger and Cyr, 2001; Overall et al., 2001; Takahashi et al., 2003a, 2003b). However, it is not known if the configuration is altered by depolymerizing or translocation. As CMTs in full-grown root hairs seem to be fixed at the cortex, it is likely that turnover is involved in reorientation of the CMTs. Indeed, it was observed that shortening after apparent contact enabled CMTs to grow in a slightly different direction.

From these results a touch-and-reorientation model is suggested in which CMTs first grow in arbitrary directions and reorient after contact with other MTs, finally resulting in the alignment of CMTs. When the MTs are less dense, the CMTs are less likely to shorten and more likely to grow undisturbed (Table II). In full-grown root hairs, this mechanism is observable as CMT density is low and dynamics relatively slow. It is possible that this type of reorientation also occurs in growing root hairs, but may be difficult to observe as the distance between the CMTs is small, which can result in reorientation at a much faster rate. During root hair growth CMTs have to follow the tip and are presumably mainly ordered in a longitudinal direction toward the root hair tip. Possibly there is a link between ion gradients at the apical root hair tip and the MTs. Bibikova et al. (1999) suggested that the action of MTs may be mediated through interactions with the cellular machinery that maintains the Ca^{2+} gradients at the tip. MTs may act in concert with actin, Rop GTPases, cell wall molecules, and plasma membrane receptors to modulate polarity in root hairs in a manner similar to what occurs in pollen tubes (for review, see Hepler et al., 2001). Starting from this mainly longitudinal orientation in growing root hairs, this touch-and-reorientation model will favor the CMTs in full-grown root hairs to align parallel to each other in the longitudinal direction and cover the whole length of the full-grown root hair. In addition the touch-and-reorientation model resulting in CMT alignment might be important to maintain root hair growth direction. Root hairs treated with taxol (MT-stabilizing drug) and oryzalin (MT-depolymerizing drug) displayed a waving growth pattern (Bibikova et al., 1999). The effects of these drugs are most likely attributable to alterations in MT dynamics. For example, taxol, widely known to induce MT stabilization and bundling (plant cells; Collings et al., 1998), specifically suppresses MT dynamics rather than stimulating directly MT polymerization or stabilization (Yvon et al., 1999). It will be challenging to analyze MT dynamics in these wavy root hairs to reveal if there is a relationship between MT dynamics and root hair growth direction.

MATERIALS AND METHODS

Plant Material and Growth Conditions

For labeling of the MTs a construct of the GFP-MBD-chimeric gene, kindly supplied by Richard Cyr (Biology Department, Pennsylvania State University) described by Marc et al. (1998) was used. The construct was cut out from a pUC18 vector, cloned in pBIN19 vector, introduced in *Agrobacterium tumefaciens* .C58 pMP90, and Arabidopsis (*Arabidopsis thaliana*) plants were transformed via in vitro root transformation (Valvekens et al., 1988) by Karimi Mansour (Flemish Interuniversity Institute for Biotechnology, Ghent, Belgium). Seeds were sterilized for 15 min in 5% sodium hypochlorite and stratified in growth medium at 4°C in the dark for 1 to 2 d. Growth medium contained Murashige and Skoog salts with 0.5% Phytagel (Sigma-Aldrich, St. Louis). Seedlings were grown at an angle of 60° during 6 d at a temperature of 21°C and 65% humidity under a photoperiod of 16 h light/ 8 h dark (50 μmol m^{-2} s^{-1}). Seedlings that were growing in the medium were selected for observation. The seedlings and the surrounding gel were cut out and transferred to one-chamber coverglasses (Labtek II from Nunc Plasticware, Naperville, IL or Microwell Dishes from Mattek, Ashland, MA). Root hairs continued to grow for several hours in these small growth chambers.

Live Cell Microscopy

A series of 3-D images (x, y, z) were recorded with a confocal laser-scanning microscope (Radiance 2000, Bio-Rad, Hertfordshire, UK), mounted on an Eclipse 300 Nikon microscope (Tokyo). A 40× S Fluor oil (NA 1.30) or 60× Plan Apo (NA 1.2) water immersion lens was used. Enhanced GFP was excited with a 488-nm line of an Argon Ion laser and detected with an HQ 528/50 nm emission filter. Simultaneous transmission images were taken to visualize the cytoplasmic architecture. A typical 3-D stack (x, y, z) consisted of 25 optical sections of whole root hairs or parts of root hairs with a separating

distance of 1 μm between the successive sections. Time lapse images were recorded automatically. Either 3-D (x, y, z) optical sections were imaged every minute resulting in 4-D datasets (x, y, z, t) or 2-D single optical sections (x, y) were imaged every second (x, y, t). The 3-D (x, y, z) optical sections were imaged with a pinhole of 1.9 airy disc units, whereas the single optical sections (x, y) were imaged with a larger pinhole of 3 airy disc units (except Supplemental Movie 2).

Drug Treatment

The MT-depolymerizing drug oryzalin (Sigma-Aldrich) was dissolved in dimethyl sulfoxide (Merck, Darmstadt, Germany) as a 10-mM stock solution and diluted in a phosphate buffered solution to a final concentration of 1 μM. The final dimethyl sulfoxide concentration did not exceed 0.01%, and this concentration had no effect on the MTs. The roots were treated by supplementing the drug solution to the Phytagel for 10 min. The drug was washed away by applying and removing buffered saline solution to the phytagel three times.

Computerized Image Analysis

All image analysis was performed with the public domain NIH ImageJ program (developed at the United States National Institutes of Health and available on the Internet at http://rsb.info.nih.gov/ij) together with a suite of purpose-written plugin programs and macros. Plugins were written for the reduction of the 3-D time lapse datasets to movies and for tracking of changes between images. They are available on request from the authors. The growth and shortening patterns of CMTs could easily be measured on the difference images (see above "Results" section; shortening = red, growth = green) in combination with the reslice tool on the movie stack. By drawing a line along the maximal length of the MT, the reslice tool gave an output of the lengths of the MTs, with the shortening and growth indicated in red and green, respectively. The density of CMTs was measured by drawing lines at well-defined distances perpendicular to the root hair axis. The plot profile of the intensities together with visual inspection made it possible to count the number of CMTs. The number of shortening events was measured by counting the significant red lines in the difference images. Root hair lengths were measured on transmission images. All movies were converted to the avi format using ImageJ. The t test (0.05) was used to measure significant differences in frequency of shortening for the different root hairs.

Upon request, all novel materials described in this publication will be made available in a timely manner for noncommercial research purposes, subject to the requisite permission from any third-party owners of all or parts of the material. Obtaining any permission will be the responsibility of the requestor.

LITERATURE CITED

Baluška F, Parker JS, Barlow PW (1992) Specific patterns of cortical and endoplasmic microtubules associated with cell growth and tissue differentiation in roots of maize (*Zea mays* L.). J Cell Sci **103:** 191–200

Baluška F, Šalaj J, Mathur J, Braun M, Jasper F, Šamaj J, Chua NH, Barlow PW, Volkmann D (2000) Root hair formation: F-actin-dependent tip growth is initiated by local assembly of profilin-supported F-actin meshworks accumulated within expansin-enriched bulges. Dev Biol **227:** 618–632

Bao YQ, Kost B, Chua NH (2001) Reduced expression of α-tubulin genes in *Arabidopsis thaliana* specifically affects root growth and morphology, root hair development and root gravitropism. Plant J **28:** 145–157

Bibikova TN, Blancaflor EB, Gilroy S (1999) Microtubules regulate tip growth and orientation in root hairs of *Arabidopsis thaliana*. Plant J **17:** 657–665

Bichet A, Desnos T, Turner S, Grandjean O, Höfte H (2001) *BOTERO1* is required for normal orientation of cortical microtubules and anisotropic cell expansion in *Arabidopsis.* Plant J **25:** 137–148

Burk DH, Liu B, Zhong RQ, Morrison WH, Ye Z-H (2001) A katanin-like protein regulates normal cell wall biosynthesis and cell elongation. Plant Cell **13:** 807–827

Cassimeris L, Pryer NK, Salmon ED (1988) Real-time observations of microtubule dynamic instability in living cells. J Cell Biol **107:** 2223–2231

Chan J, Calder GM, Doonan JH, Lloyd CW (2003) EB1 reveals mobile microtubule nucleation sites in *Arabidopsis.* Nat Cell Biol **5:** 967–971

Chytilova E, Macas J, Sliwinska E, Rafelski SM, Lambert GM, Galbraith DW (2000) Nuclear dynamics in *Arabidopsis thaliana.* Mol Biol Cell **11:** 2733–2741

Cleary AL, Hardham AR (1987) Depolymerization of microtubule arrays in root tip cells by oryzalin and their recovery with modified nucleation patterns. Can J Bot **66:** 2353–2366

Collings DA, Asada T, Allen NS, Shibaoka H (1998) Plasma membrane-associated actin in bright yellow 2 tobacco cells: evidence for interaction with microtubules. Plant Physiol **118:** 917–928

Cyr RJ (1994) Microtubules in plant morphogenesis: role of the cortical array. Annu Rev Cell Biol **10:** 153–180

de Ruijter NCA, Rook MB, Bisseling T, Emons AMC (1998) Lipochito-oligosaccharides re-initiate root hair tip growth in *Vicia sativa* with high calcium and spectrin-like antigen at the tip. Plant J **13:** 341–350

Desai A, Mitchinson TJ (1997) Microtubule polymerization dynamics. Annu Rev Cell Dev Biol **13:** 83–117

Dhonukshe P, Gadella TWJ Jr (2003) Alteration of microtubule dynamic instability during preprophase band formation revealed by yellow fluorescent protein-CLIP170 microtubule plus-end labeling. Plant Cell **15:** 597–611

Dolan L, Duckett CM, Grierson C, Linstead P, Schneider K, Lawson E, Dean C, Poethig S, Roberts K (1994) Clonal relationships and cell patterning in the root epidermis of *Arabidopsis.* Development **120:** 2465–2474

Emons AMC, Derksen J (1986) Microfibrils, microtubules and microfilaments of the trichoblast of *Equisetum hyemale.* Acta Bot Neerl **35:** 311–320

Erhardt M, Stoppin-Mellet V, Campagne S, Canaday J, Mutterer J, Fabian T, Sauter M, Muller T, Peter C, Lambert A-M, et al (2002) The plant Spc98p homologue colocalizes with γ-tubulin at microtubule nucleation sites and is required for microtubule nucleation. J Cell Sci **115:** 2423–2431

Galway ME, Heckman JW Jr, Schiefelbein JW (1997) Growth and ultrastructure of *Arabidopsis* root hairs: the *rhd3* mutation alters vacuole enlargement and tip-growth. Planta **201:** 209–218

Geitmann A, Emons AMC (2000) The cytoskeleton in plant and fungal cell tip growth. J Microsc (Oxf) **198:** 218–245

Granger CL, Cyr RJ (2001) Spatiotemporal relationships between growth and microtubule orientation as revealed in living root cells of *Arabidopsis thaliana* transformed with green-fluorescent-protein gene construct GFP-MBD. Protoplasma **216:** 201–214

Hasezawa S, Ueda K, Kumugai F (2000) Time-sequence observations of microtubule dynamics throughout mitosis in living cell suspensions of stable transgenic *Arabidopsis*: direct evidence for the origin of cortical microtubules at the M/G(1) interface. Plant Cell Physiol **41:** 244–250

Hepler PK, Vidali L, Chueng AY (2001) Polarized cell growth in higher plants. Annu Rev Cell Dev Biol **17:** 159–187

Hush JM, Overall L (1996) Cortical microtubule reorientation in higher plants: dynamics and regulation. J Microsc (Oxf) **181:** 129–139

Hush JM, Wadsworth P, Callaham DA, Hepler PK (1994) Quantification of microtubule dynamics in living plant cells using fluorescence redistribution after photobleaching. J Cell Sci **107:** 775–784

Hussey PJ, Hawkins TJ, Igarashi H, Kaloriti D, Smertenko A (2002) The plant cytoskeleton: recent advances in the study of the plant microtubule-associated proteins MAP-65, MAP-190 and the Xenopus MAP215-like protein, MOR1. Plant Mol Biol **50:** 915–924

Janson ME, de Dood ME, Dogterom M (2003) Dynamic instability of microtubules is regulated by force. J Cell Biol 161: 1029–1034

Justus CD, Anderhag P, Goins JL, Lazzaro MD (2004) Microtubules and micofilaments coordinate to direct a fountain streaming pattern in elongating conifer pollen tube tips. Planta 219: 103–109

Ketelaar T, de Ruijter NCA, Emons AMC (2003) Unstable F-actin specifies the area and microtubule direction of cell expansion in Arabidopsis root hairs. Plant Cell 15: 285–292

Ketelaar T, Faivre-Moskalenko C, Esseling JJ, de Ruijter NCA, Grierson CS, Dogterom M, Emons AMC (2002) Positioning of nuclei in Arabidopsis root hairs: an actin regulated process of tip growth. Plant Cell 14: 2941–2955

Kline-Smith SL, Walczak CE (2002) The microtubule-destabilizing kinesin XKCM1 regulates microtubule dynamic instability in cells. Mol Biol Cell 13: 2718–2731

Kropf DL, Bisgrove SR, Hable WE (1998) Cytoskeletal control of polar growth in plant cells. Curr Biol 10: 117–122

Lambert AM, Lloyd CW (1994) The higher plant microtubule cycle. In JS Hyams, CW Lloyd, eds, Microtubules. John Wiley & Sons, New York, pp 325–341

Lloyd C (1983) Helical microtubular arrays in onion root hairs. Nature 305: 311–313

Lloyd C, Hussey P (2001) Microtubule-associated proteins in plants: why we need a MAP. Nat Rev Mol Cell Biol 2: 40–47

Lloyd C, Pearce KJ, Rawlins DJ, Ridge RW, Shaw PJ (1987) Endoplasmic microtubules connect the advancing nucleus to the tip of legume root hairs, but F-actin is involved in basipetal migration. Cell Motil Cytoskeleton 8: 27–36

Marc J, Granger CL, Brincat J, Fisher DD, Kao TH, McCubbin AG, Cyr RJ (1998) A GFP-MAP4 reporter gene for visualizing cortical microtubule rearrangements in living epidermal cells. Plant Cell 10: 1927–1939

Mathur J, Chua NH (2000) Microtubule stabilization leads to growth reorientation in Arabidopsis trichomes. Plant Cell 12: 465–477

Mayer U, Jürgens G (2002) Microtubule cytoskeleton: a track record. Curr Opin Plant Biol 5: 494–501

Miller DD, de Ruijter NCA, Bisseling T, Emons AMC (1999) The role of actin in root hair morphogenesis: studies with lipochito-oligosaccharide as a growth stimulator and cytochalasin as an actin perturbing drug. Plant J 17: 141–154

Miller DD, de Ruijter NCA, Emons AMC (1997) From signal to form: aspects of the cytoskeleton-plasma membrane-cell wall continuum in root hair tips. J Exp Bot 48: 1881–1896

Mizuno K (1993) Microtubule-nucleation sites on nuclei of higher plant cells. Protoplasma 173: 77–85

Overall RL, Dibbayawan TP, Blackman LM (2001) Intercellular alignments of Plant cytoskeleton. J Plant Growth Regul 2: 162–169

Pierson ES, Miller DD, Callaham DA, vanAken D, Hackett G, Hepler PK (1996) Tip-localized calcium entry fluctuates during pollen tube growth. Dev Biol 174: 160–173

Schiebel E (2000) γ-tubulin complexes: binding to the centrosome, regulation and microtubule nucleation. Curr Opin Cell Biol 12: 113–118

Schmit A-C (2002) Acentrosomal microtubule nucleation in higher plants. Int Rev Cytol 220: 257–289

Schnepf E (1986) Cellular polarity. Annu Rev Plant Physiol 37: 23–47

Shaw SL, Kamyar R, Erhardt DW (2003) Sustained microtubule treadmilling in Arabidopsis cortical arrays. Science 300: 1715–1718

Sieberer B, Emons AMC (2000) Cytoarchitecture and pattern of cytoplasmic streaming in developing root hairs of Medicago truncatula and during deformation by Nod factors. Protoplasma 214: 118–127

Sieberer B, Timmers ACJ, Lhuissier FGP, Emons AMC (2002) Endoplasmic microtubules configure the sub-apical cytoplasm and are required for fast growth of Medicago trunculata root hairs. Plant Physiol 130: 977–988

Stoppin V, Vantard M, Schmit AC, Lambert AM (1994) Isolated plant nuclei nucleate microtubule assembly: the nuclear surface in higher plants has centrosome-like activity. Plant Cell 6: 1099–1106

Stoppin-Mellet V, Gaillard J, Vantard M (2002) Functional evidence for in vitro microtubule severing by the plant katanin homolog. Biochem J 365: 337–342

Takahashi H, Hirota K, Kawahara A, Hayakawa E, Inoue Y (2003a)
Randomization of cortical microtubules in root epidermal cells induces root hair initiation in Lettuce (Lactuca sativa L.) seedlings. Plant Cell Physiol 44: 350–359

Takahashi H, Kawahara A, Inoue Y (2003b) Ethylene promotes the induction by auxin of the cortical microtubule randomization required for low-pH-induced root hair initiation in Lettuce (Lactuca sativa L.) seedlings. Plant Cell Physiol 44: 932–940

Tominaga M, Morita K, Sonobe S, Yokata E, Shimmen T (1997) Microtubules regulate the organization of actin filaments at the cortical region in root hair cells of Hydrocharis. Protoplasma 199: 83–92

Tournebize R, Popov A, Kinoshita K, Ashford AJ, Rybina S, Pozniakovsky A, Mayer TU, Walczak CE, Karsenti E, Hyman AA (2000) Control of microtubule dynamics by the antagonistic activities of XMAP215 and XKCM1 in Xenopus egg extracts. Nat Cell Biol 2: 13–19

Valvekens D, Van Montagu M, Van Lijsebettens M (1988) Agrobacterium tumefaciens-mediated transformation of Arabidopsis thaliana root explants by using kanamycin selection. Proc Natl Acad Sci USA 85: 5536–5540

Van Bruaene N, Joss G, Thas O, Van Oostveldt P (2003) Four-dimensional imaging and computer-assisted track analysis of nuclear migration in root hairs of Arabidopsis thaliana. J Microsc (Oxf) 211: 167–178

Vorobjev IA, Rodionov VI, Maly IV, Borisy GG (1999) Contribution of plus and minus end pathways to microtubule turnover. J Cell Sci 112: 2277–2289

Vos JW, Dogterom M, Emons AMC (2004) Microtubules become more dynamic but not shorter during preprophase band formation: a possible "search-and-capture" mechanism for microtubule translocation. Cell Motil Cytoskeleton 57: 246–258

Walczak CE, Mitchinson TJ, Desai A (1996) XKCM1: a Xenopus kinesin-related protein that regulates microtubule dynamics during mitotic spindle assembly. Cell 84: 37–47

Wasteneys GO (2002) Microtubule organization in the green kingdom: chaos or self-order? J Cell Sci 115: 1345–1354

Wasteneys GO, Galway ME (2003) Remodelling the cytoskeleton for growth and form: an overview with some new views. Annu Rev Plant Biol 54: 691–722

Wasteneys GO, Gunning BES, Hepler PK (1993) Microinjection of fluorescent brain tubulin reveals dynamic properties of cortical microtubules in living plant cells. Cell Motil Cytoskeleton 24: 205–213

Wasteneys GO, Jablonsky PP, Williamson RE (1989) Assembly of purified brain tubulin at cortical and endoplasmic sites in perfused internodal cells of the alga Nitella tasmanica. Cell Biol Int Rep 13: 513–528

Wasteneys GO, Williamson RE (1989a) Reassembly of microtubules in Nitella tasmanica: assembly of cortical microtubules in branching clusters and its relevance to steady-state microtubule assembly. J Cell Sci 93: 705–714

Wasteneys GO, Williamson RE (1989b) Reassembly of microtubules in Nitella tasmanica: quantitaive analysis of assembly and orientation. Eur J Cell Biol 50: 76–83

Webb M, Jouannic S, Foreman J, Linstead P, Dolan L (2002) Cell specification in the Arabidopsis root epidermis requires the activity of ECTOPIC ROOT HAIR 3: a katanin-p60 protein. Development 129: 123–131

Weerasinghe RR, Collings DA, Johannes E, Allen NS (2003) The distributional changes and role of microtubules in Nod factor-challenged Medicago sativa root hairs. Planta 218: 276–287

Whittington AT, Vugrek O, Wei KJ, Hasenbein NG, Sugimoto K, Rashbrooke MC, Wasteneys GO (2001) MOR1 is essential for organizing cortical microtubules in plants. Nature 411: 610–613

Wymer CL, Bibikova TN, Gilroy S (1997) Cytoplasmic free calcium distributions during the development of root hairs of Arabidopsis thaliana. Plant J 12: 427–439

Yang ZB (1998) Signaling tip growth in plants. Curr Opin Plant Biol 1: 525–530

Yvon A-MC, Wadsworth P, Jordan MA (1999) Taxol suppresses dynamics of individual microtubules in living human tumor cells. Mol Biol Cell 10: 947–959

Zhang DH, Wadsworth P, Hepler PK (1990) Microtubule dynamics in living dividing plant cells: confocal imaging of microinjected fluorescent brain tubulin. Proc Natl Acad Sci USA 87: 8820–8824